SPE-173202-MS

Numerical Simulation of Three-Hydrocarbon-Phase Flow with Robust Phase Identification

Zhongguo Xu, and Ryosuke Okuno, University of Alberta

This paper was prepared for presentation at the SPE Reservoir Simulation Symposium held in Houston, Texas, USA, 23–25 February 2015.

Abstract

Low-temperature oil displacement by enriched-gas or carbon-dioxide (CO_2) can exhibit multiphase flow of three hydrocarbon phases; the oleic (L_1), solvent-rich liquid (L_2), and gaseous (V) phases. The L_2 phase can play a significant role in these oil recovery processes. Recently, oil displacement by three hydrocarbon phases was explained on the basis of interphase mass transfer on phase transitions in multiphase flow. However, systematic investigation into the complex interplay between phase behavior and mobilities has been hindered by issues in multiphase compositional flow simulation, such as incorrect phase identification.

This paper presents the effect of relative permeability on oil displacement by three hydrocarbon phases. A new method for robust phase identification is developed and implemented in a 1D convective flow simulator with no volume change on mixing. The new method uses tie triangles and their normal unit vectors tabulated as part of the simulation input information. The extensions of the limiting tie triangles at the upper and lower critical endpoints (UCEP and LCEP) define three different regions in composition space; the super-UCEP, super-LCEP, and sub-CEP regions. The method can properly recognize five different two-phase regions surrounding the three-phase region; the two two-phase regions that are super-CEP, and the three different two-phase regions that originate with the corresponding edges of the three-phase region in the sub-CEP region. Multiphase behavior calculations are conducted rigorously by use of the Peng-Robinson equation of state with the van der Waals mixing rules during the flow simulation. Simulation case studies are presented with a quaternary model and the West Sak oil model with 15 components.

Results show that the phase-identification method developed in this research can correctly solve for phase identities in three-hydrocarbon-phase flow simulation. The method can quantify the relative location of the current overall composition to the three-phase region in composition space. Simulation results are analyzed by use of the distance parameters that describe interphase mass transfer on multiphase transitions in oil displacement. In the case study for the West Sak oil displacement, the analysis confirms that the miscibility level of oil displacement increases with increasing methane dilution. The effect of relative permeability diminishes as the miscibility level increases owing to methane dilution. The distance parameters can properly represent the interaction of phase behavior and mobilities since they are derived from mass conservation, not only from thermodynamic conditions.

Introduction

Multiphase behavior can occur in various oil-recovery processes, such as gas injection, water-alternating-gas injection, steam injection, and steam-solvent coinjection. For example, three-hydrocarbon-phase behavior has been observed in static experiments and slimtube tests for enriched-gas and CO_2 floods at relatively low reservoir temperatures (Metcalfe and Yarborough 1979; Gardner et al. 1981; Orr and Jensen 1984; Creek and Sheffield 1993). These phases are the V, L_1, and L_2 phases. Also, steam injection for heavy oil and steam-solvent coinjection for bitumen involve at least three phases with mutual solubilities; i.e., the V, L_1, and aqueous phases (Glandt and Chapman 1995; Luo and Barrufet 2005). Further complication in the coinjection may arise due to the L_2-phase appearance and asphaltene precipitation/deposition. Theory of oil displacement in multiphase flow is important for designing these processes. Development of such theory requires analytical and numerical solutions of multiphase flow (LaForce et al. 2008ab; Bruining and Marchesin 2007), but the complicated interplay between multiphase behavior and isothermal/non-isothermal flow can make robust solution of multiphase flow difficult.

Oil displacements in three-hydrocarbon-phase flow during enriched-gas and CO_2 floods were studied by Okuno et al. (2011) and Okuno and Xu (2014ab) by use of UTCOMP, an equation-of-state (EOS) compositional multiphase reservoir simulator developed at the University of Texas at Austin (Chang 1990; Chang et al. 1990). Okuno et al. (2011) concluded that low-temperature oil displacement by CO_2 can be efficient when the composition path traverses near the upper and lower critical endpoints (CEPs). A CEP is a critical state in which two of the three equilibrium phases become critical. The three-hydrocarbon-phase behavior is bounded by two types of critical endpoints (CEPs) in composition space (Appendix A). The lower CEP (LCEP) is a tie line (or a limiting tie triangle) in which the L_1 and L_2 phases merge in the presence of the V phase. The upper CEP (UCEP) is a tie line (or a limiting tie triangle) in which the L_2 and V phases merge in the presence of the L_1 phase.

Okuno and Xu (2014a) presented a detailed analysis of mass conservation on multiphase transitions between two and three phases in three-hydrocarbon-phase flow (see Appendix B for schematics of phase behavior in two- and three-phase displacements). Analytical conditions were derived to describe how components should be redistributed among phases (i.e., interphase mass transfer) on multiphase transitions for efficient oil displacement by three phases (Appendix C). The derived conditions were successfully applied to explain several oil displacements that exhibited nonmonotonic oil recovery with respect to pressure or gas enrichment at a given throughput. The cases studied include the West Sak oil displacement by enriched gas, for which slimtube experiments showed that oil recovery at 1.2 pore-volumes injected (PVI) first decreased, then increased, and finally decreased again with decreasing gas enrichment (DeRuiter et al. 1994; Mohanty et al. 1995).

Okuno and Xu (2014b) further studied the interphase mass transfer for multicontact miscibility (MCM) development between the L_1 and L_2 phases in three-hydrocarbon-phase flow. Their analysis indicated that MCM between L_1 and L_2 can be developed as the distance parameters (see Equations C-6, C-7, and C-8) diminish. This MCM development can occur on a LCEP tie line, where the non-V phase switches its identity from L_1 to L_2 with no three-phase equilibrium involved. This can be interpreted as the limiting three-phase flow, where the L_1 phase is completely displaced by the L_2 phase. They did not study the thermodynamic MCM that might occur at a tricritical point of three hydrocarbon phases. Okuno (2009) calculated a tricritical point when UCEP and LCEP merged in composition space [i.e., an unsymmetrical tricritical point (Knobler and Scott 1984)] for a quaternary system made after the Bob Slaughter Block oil with CO_2. That is, the three-phase region had disappeared when the tricritical point appeared in composition space.

The multiphase interaction in three-phase flow should be understood more systematically to create useful knowledge for enhanced oil recovery. The experimental results of DeRuiter et al. (1994) and Mohanty et al. (1995) clearly indicate that methane dilution can substantially affect the propagation of

dense solvent components that should effectively contact the reservoir oil in situ. The prior numerical research on three-hydrocarbon-phase flow was conducted with several different fluids by use of UTCOMP with its robust phase-behavior calculations. However, the research was limited in terms of thermodynamic and flow conditions. For example, how phase mobilities affect the interphase mass transfer was not studied in detail, due to the lack of robust phase identification in EOS compositional simulation (Mohanty et al. 1995; Yuan and Pope 2012; Beygi et al. 2014). Phase identification is always part of the solution of a multiphase flow problem, and is usually required to assign relative permeabilities to phases in simulation. Also, simulations by use of UTCOMP with a conventional relative permeability model were not always possible depending on the thermodynamic conditions set, as mentioned in Okuno and Xu (2014b). This hindered more comprehensive investigation for systematic understanding of multiphase flow.

This paper is concerned with numerical solutions of 1D three-hydrocarbon-phase convective flow problems set by temperature, pressure, initial and injection compositions, fluid properties, and relative permeabilities. To study the interplay between multiphase behavior and phase mobilities in three-hydrocarbon-phase flow, a new method is developed for robust phase identification and implemented in a 1D multiphase convective flow simulator. The new method is compared with the conventional method for phase identification (Perschke et al. 1989). In case studies, the simulator with the new phase-identification method is used to investigate the effect of relative permeability parameters on oil displacement by three hydrocarbon phases. Results confirm that the distance parameters of Okuno and Xu (2014ab) are capable of considering not only the effect of miscibility (i.e., phase behavior), but also the effect of relative permeability (i.e., multiphase flow) on oil displacement by three phases.

Formulation and Solution Methods

Theory of gas injection has been established on the basis of 1D multicomponent convective flow (Johns 1992; Dindoruk 1992; Orr 2007). Equation C-1 is often used for analytical and numerical solutions of gas injection problems (Helfferich 1979; Lake 1989; Johns 1992; LaForce and Johns 2005ab; LaForce et al. 2006; Orr 2007; LaForce et al. 2008ab; LaForce and Orr 2008; LaForce and Johns 2009; LaForce and Jessen 2010; LaForce 2012). In this research, the corresponding finite-difference equations (Equation C-3) are solved explicitly by use of the single-point upstream weighting for the flux term, as described in Johns (1992) and Orr (2007). The advantage of not having to solve for gridblock pressures is important in terms of computational robustness and costs in this research. A multiphase flow problem in this research is defined by temperature, pressure, initial and injection compositions, fluid properties, and relative permeability parameters. A solution consists of the compositions, amounts, and identities of equilibrium phases as functions of dimensionless velocity (or time in PVI and dimensionless distance from the injector).

The thermodynamic model used is the Peng-Robinson (PR) EOS (Peng and Robinson 1976) with the van der Waals mixing rules. Phase viscosities are calculated with the correlation of Lohrenz et al. (1964). The multiphase behavior algorithms used are based on Perschke (1988) and Chang (1990) for sequential flash and stability calculations and Okuno et al. (2010) for constant-K flash.

The relative permeability model of Corey et al. (1956) is used for simplicity. Yuan and Pope (2012) stated that the Corey model follows the trends of experimental relative permeability data. Yuan and Pope (2012) proposed a novel relative permeability model, which is continuous in multicomponent composition space. They implemented the model in the UTCOMP simulator to demonstrate the improved robustness of multiphase flow simulation. However, the relationship between composition and relative permeability is not fully understood. The phase-identification method presented in this research is not dependent on the relative permeability model used. If discontinuities are present in the correct solution of a multiphase flow problem for any reason (e.g., due to the relative permeability model used), they are solved for as they are.

The conventional method for phase identification was developed by Perschke et al. (1989). In their

method, the L_1 phase in a three-phase region of L_1-L_2-V was the one with the highest concentration of the heaviest hydrocarbon component. Of the two remaining phases, the denser phase was labeled as L_2, and the less dense phase was V. For two equilibrium phases, in which the L_1 phase was assumed to exist, the L_1 phase was labeled by use of the logic mentioned previously. The other phase was labeled as either V or L_2 depending on the mass density of that phase. If the mass density of the phase was lower than a specified threshold value, it was labeled as V. Otherwise, it was labeled as L_2. It was not entirely clear in their paper how to handle the V-L_2 equilibrium that can occur near the injection composition in enriched-gas and CO_2 injection simulations at low temperature (Okuno and Xu 2014b). A single phase was labeled by the user on the basis of the phase behavior data available.

The conventional method described in the preceding paragraph has been used for decades, but it has been a difficult problem to assign physically correct identities to equilibrium phases (Yuan and Pope 2012). Particularly, the use of a fixed mass-density threshold is known to be problematic for phase labeling in a two-phase region in three-hydrocarbon-phase flow simulation (Mohanty et al. 1995; Li et al. 2014; Beygi et al. 2014). This type of failures will be shown in cases studied in this paper. The use of mass densities by Perschke et al. (1989) for three-phase labeling is less problematic. However, it is somewhat inconsistent to use volumetric predictions for identifying equilibrium phases, the compositions of which are determined by the geometry of the Gibbs free energy. This is because the two types of predictions (i.e., volumetric and compositional behavior) are not entirely coherent in the conventional phase–behavior modeling scheme based on a cubic EOS. This becomes obvious when volume shift is used to adjust volumetric predictions in fluid characterization (Kumar and Okuno 2013). It will be more robust if phase identification can be based primarily on compositional predictions in simulation. Note, however, that density information may be still useful in some special cases, such as the identification of the aqueous (condensed water) and vapor (steam) phases in steam injection simulation for dead heavy oil.

A fundamental reason for the difficulty, especially in two-phase identification, comes from the fact that the identity of a phase is defined in comparison with other phases calculated by the thermodynamic model used. Robust phase identification requires knowledge of phase equilibria calculated away from the thermodynamic conditions of interest. In this research, three-hydrocarbon-phase flow simulation at a fixed pressure and temperature uses a tie-triangle table that contains a few tie triangles and their normal unit vectors, as part of the simulation input information. The limiting tie triangle at a CEP, if present, is always tabulated together with its normal unit vector. For example, a tie-triangle table for composition space that contains the entire three-phase region (as shown in Figure A-1) includes the two limiting tie triangles for the UCEP and LCEP.

The extensions of these limiting tie triangles define three different regions in composition space; i.e., the super-UCEP, super-LCEP, and sub-CEP regions. In the super-UCEP region, two equilibrium phases are considered to originate with the UCEP tie line, L_1-L_2=V, and denoted as the L_1 and (L_2V) phases. In the super-LCEP region, two equilibrium phases are considered to originate with the LCEP tie line, L_1=L_2-V, and denoted as the V and (L_1L_2) phases. In the sub-CEP region, there are three different two-phase regions; i.e., L_1-V, L_1-L_2, and L_2-V. They originate with their corresponding edges of three phases. Altogether, five different two-phase regions can be recognized around the three-phase region in composition space.

When three equilibrium phases are calculated in simulation in this research, the phase with the highest concentration of the heaviest hydrocarbon component is labeled as L_1, as in Perschke et al. (1989). The phase with the highest methane concentration is labeled as V because it is unlikely that methane/hydrocarbon mixtures form three hydrocarbon phases at realistic reservoir temperature (Peters 1994). The other phase is labeled as L_2. Unlike the method of Perschke et al. (1989), phase mass densities are not used for labeling V and L_2 in a three-phase region. Note that the L_1-V edge is not always the longest edge of a tie triangle of L_1-L_2-V in multicomponent composition space. That is, it is not robust to use lengths of tie-triangle edges for three-phase identification.

Phase identification in a two-phase region in this research is substantially different from that in Perschke et al. (1989). N_T tie triangles are tabulated from the UCEP tie triangle through the LCEP tie triangle. The normal vectors for the N_T tie triangles point from the UCEP to LCEP in this research. Two-phase identification starts with calculation of dot products using the UCEP and LCEP tie triangles as

$$d^{UCEP} = (\vec{z} - \vec{x}_{\bullet}^{UCEP}) \cdot \vec{n}^{UCEP} \quad (1)$$

$$d^{LCEP} = (\vec{z} - \vec{x}_{\bullet}^{LCEP}) \cdot \vec{n}^{LCEP}, \quad (2)$$

where $\vec{z}$ is the vector of the current overall composition, and $\vec{n}$ is the unit normal vector. $\vec{x}_{\bullet}$ is the composition vector of one of the three phases, which can be either L_1, L_2, or V, but should be used consistently. Superscripts UCEP and LCEP indicate that they are associated with the UCEP and LCEP tie triangles, respectively. If the two dot products are both negative, the overall composition is in the super-UCEP region; the current two phases are the L_1 and (L_2V) phases. If the two dot products are both positive, the overall composition is in the super-LCEP region; the current two phases are the V and (L_1L_2) phases. If d^{UCEP} is positive and d^{LCEP} is negative, the overall composition is in the sub-CEP region.

Table 1—COREY RELATIVE PERMEABILITY PARAMETERS FOR 1D OIL DISPLACEMENT SIMULATIONS

Yuan and Pope (2012)	Phase index	L_1	V	L_2
	Residual saturation	0.2	0.2	0.2
	Endpoint	0.2	1.0	0.4
	Exponent	2	2	2
Model 1	Phase index	L_1	V	L_2
	Residual saturation	0.2	0.2	0.2
	Endpoint	0.2	1.0	1.0
	Exponent	2	2	2
Model 2	Phase index	L_1	V	L_2
	Residual saturation	0.2	0.2	0.2
	Endpoint	0.2	1.0	0.2
	Exponent	2	2	2

If the overall composition in a two-phase region is calculated to be in the sub-CEP region, the following dot products are calculated for the other ($N_T - 2$) tie triangles tabulated:

$$d^m = (\vec{z} - \vec{x}_{\bullet}^m) \cdot \vec{n}^m \quad (3)$$

for $2 \le m \le (N_T - 1)$, where m is the index for the tabulated tie triangles. Note that d^1 ($= d^{UCEP}$) is positive and d^{N_T} ($= d^{LCEP}$) is negative. Then, we find two tie triangles, m+ and m-, from the table such that

$$d^{m+} = \min_m\{d^m : d^m > 0\} \quad (4)$$

$$d^{m-} = \max_m\{d^m : d^m < 0\}. \quad (5)$$

Linear interpolation of three phase compositions is conducted between the two tie triangles m+ and m- as follows:

$$\vec{x}_j = \left(|d^{m-}|\vec{x}_j^{m+} + d^{m+}\vec{x}_j^{m-}\right)/(d^{m+} + |d^{m-}|), \quad (6)$$

where $j = \{L_1, L_2, V\}$. Finally, negative flash by use of the algorithm of Okuno et al. (2010) with $\vec{z}$ and K values from the interpolated $\vec{x}_j$ is performed to determine in which region the current overall composition is, L_1-L_2, L_1-V, or L_2-V. The negative constant-K flash indicates the phase identities of the two phases if a sufficient N_T is used. In a single-phase region, the procedure is identical with that of Perschke et al. (1989), which is based on the user's input.

If composition space does not contain the entire three-phase region, the N_T triangles to be tabulated are selected from positive composition space. For example, if the UCEP is not present in positive composition space, the first triangle is a triangle on a subspace of ($N_C - 1$) components. If no CEPs are present in positive composition space, the first and N_T^{th} triangles are taken from two different subspaces of ($N_C - 1$) components that contain subcritical three phases.

It is theoretically conceivable that d^{UCEP} is negative and d^{LCEP} is positive when the trajectory of $\vec{n}$ is

Table 2—FLUID PROPERTIES FOR THE QUATERNARY MODEL (Okuno and Xu 2014a)

	Oil (Mole %)	Gas (Mole %)	Molecular Weight	Tc (°R)	Pc (psia)	Acentric Factor	Vc (ft^3/lb-mol)
PC1	37.22	20	17.268	357.77	666.48	0.0193	1.6763
PC2	10.63	80	40.288	630.32	656.22	0.1402	2.9740
PC3	30.11	0	352.25	1318.10	240.31	0.5574	21.572
PC4	22.04	0	1052.00	1967.30	94.80	1.1313	83.571

substantially non-linear in multicomponent composition space. However, this has not been observed so far; the extensions of the two CEP tie triangles intersect in negative composition space in the cases tested in our research.

An appropriate value for N_T is dependent on the level of non-linearity of the $\vec{n}$ trajectory and the number of components used in simulation. The case studies section will show that a larger N_T tends to be required for a larger N_C.

Table 3—BINARY INTERACTION PARAMETERS FOR THE QUATERNARY SYSTEM

Components	PC1	PC2	PC3	PC4
PC1	0			
PC2	0.0052	0		
PC3	0	0.005	0	
PC4	0.1822	0.1336	0	0

Perschke et al. (1989) also described the phase tracking technique that labels phases in simulation on the basis of the concentrations of a selected component in the tracked phases from the previous time step. The phases at the new time step are labeled such that the concentrations are closest to the values at the old time step. This phase tracking technique can offer time savings in simulation by skipping the more careful phase identification described in this section. In this research, however, no phase tracking is performed because the primary interest is in obtaining correct numerical solutions of multiphase displacements, instead of computational speed.

As mentioned earlier in this section, use of tie triangles tabulated prior to simulation is effective in improving the phase identification issues because a two-phase region originates with an edge of the corresponding tie triangle in composition space. This global characteristic of thermodynamic problems (which cannot be solved robustly only from local information) can be also seen in multiphase flash; i.e., global minimization of the Gibbs free energy. Use of tie simplex information tabulated prior to simulation has been shown to be effective in speeding up fully implicit reservoir simulations (Voskov and Tchelepi 2009ab; Iranshahr et al. 2012, 2013).

Case Studies

Two simulation cases are presented to show the effect of relative permeability on oil displacement by three hydrocarbon phases and the improved phase-identification method in comparison with the conventional method by Perschke et al. (1989). The first case uses a quaternary fluid model, and the second case uses a 15-component fluid model, in which displacements occur in composition space of much higher dimensions. The 1D convective flow simulator described in the preceding section and Appendix C is used with 1000 gridblocks. The gridblock size is uniform, and $\Delta t_D/\Delta x_D$ is constant at 0.05. The porosity and permeability are 20% and 1000 mD, respectively, as in Okuno and Xu (2014a). The Corey relative permeability parameters used are taken from Yuan and Pope (2012), in which the endpoint relative permeabilities for the V and L_2 phases are markedly different from each other (Table 1). Thus, correct phase identification is required to simulate these cases. As shown in Table 1, two models are prepared for relative permeabilities; the L_2 phase shares the same parameter values with the V phase in model 1 and with the L_1 phase in model 2.

The phase-identification algorithm described in the preceding section can properly distinguish the super-CEP states from the sub-CEP states. It would be reasonable to consider composition-dependent

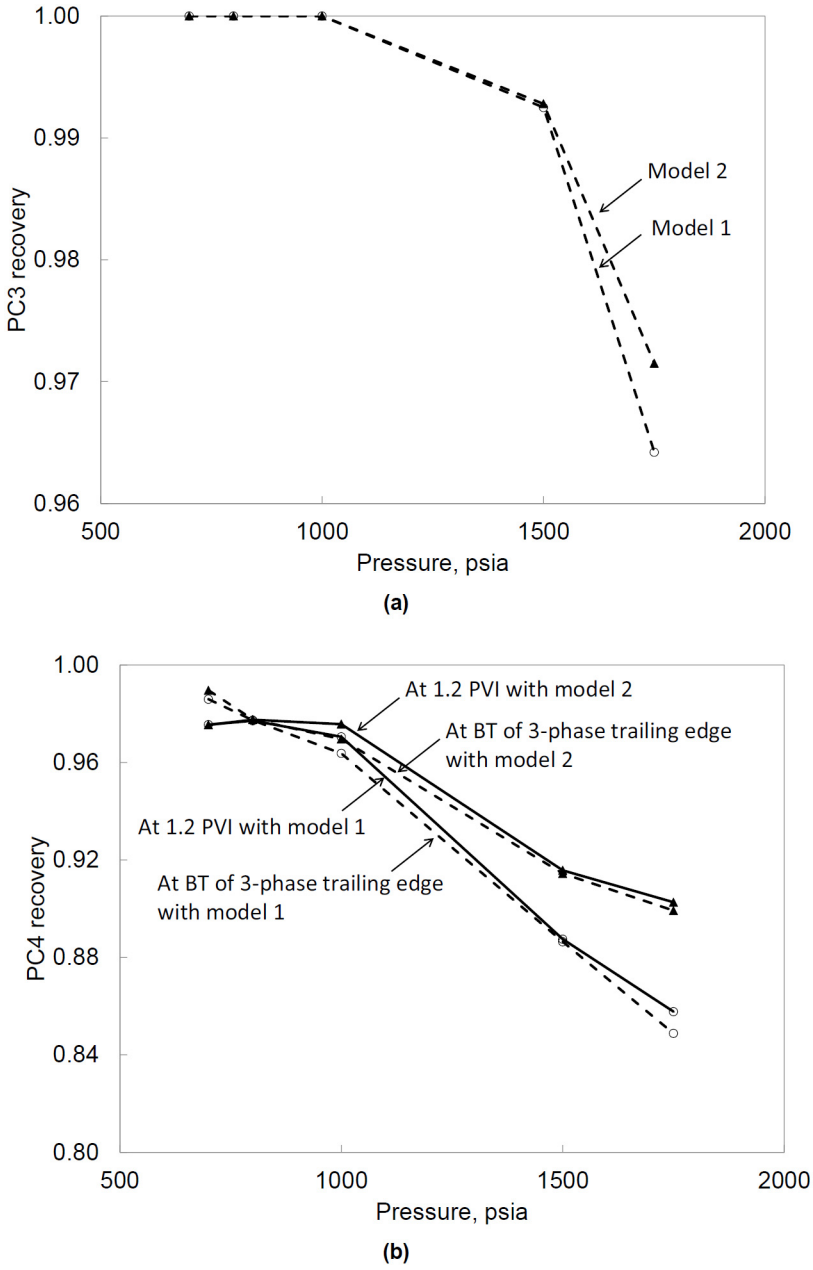

Figure 1—Simulated recoveries of PC3 and PC4 in the quaternary displacement at 86°F; (a) PC3 recoveries at breakthrough (BT) of the trailing edge of three phases, and (b) PC4 recoveries at 1.2 PVI and BT of the trailing edge of three phases. PC3 recoveries at 1.2 PVI are 100% with the two models, and are not shown. The Corey relative permeability parameters used are listed in Table 1. The components' properties are given in Tables 2 and 3. The miscibility level of oil displacement increases with decreasing pressure. The PC4 recovery at BT of the three-phase trailing edge is calculated to be approximately 5% higher with model 2 than with model 1.

relative permeability for the five types of two-phase regions. For example, the code developed in this research can model the relative permeability parameters for the (L_2V) phase in a super-UCEP region as functions of those for the L_2 and V phases at sub-CEP states. In this section, however, the relative-permeability parameters for the L_1 and L_2 phases are used in a super-UCEP region, and those for the L_1 and V phases are used in a super-LCEP region.

Quaternary Displacement

The quaternary fluid used was taken from Okuno and Xu (2014a), which was made after the Schrader Bluff oil model of Guler et al. (2010). The four components consist of one light pseudocomponent (PC1),

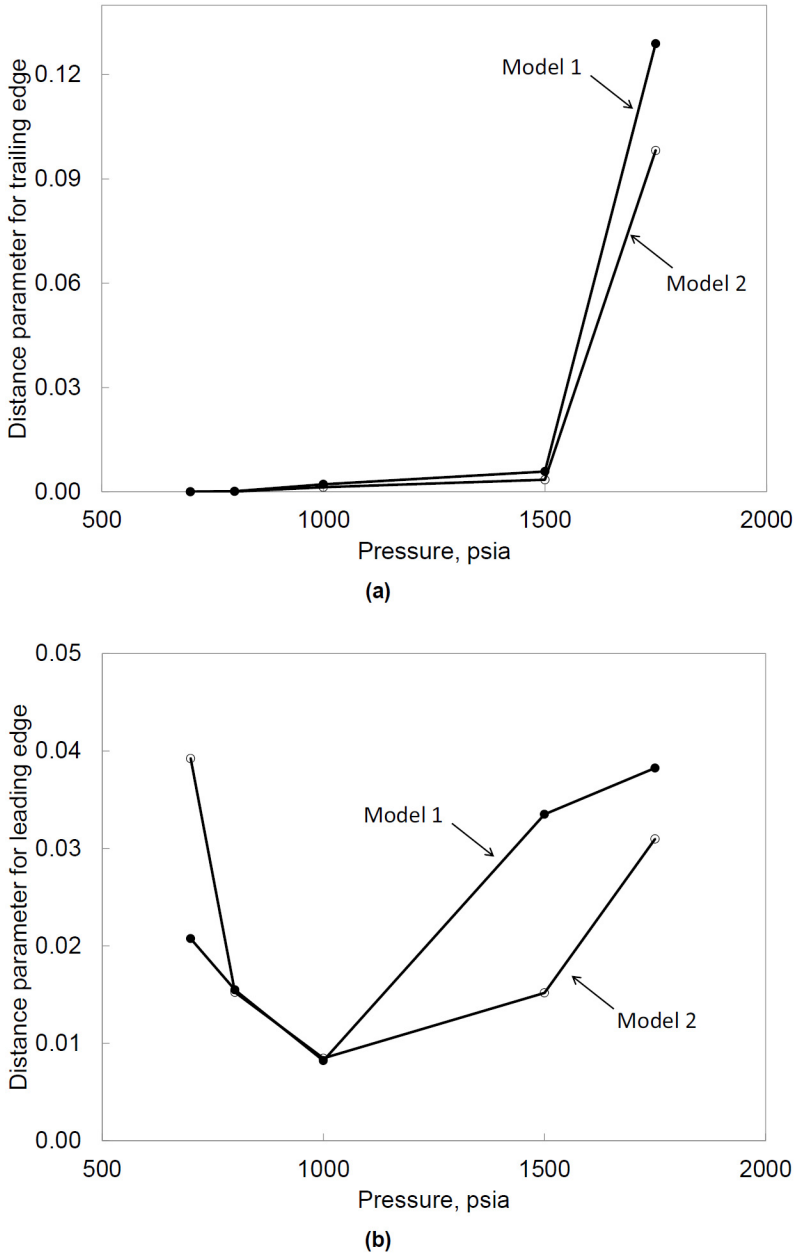

Figure 2—The δ^T and d^L parameters (see Appendix C) for the quaternary displacements with relative permeability models 1 and 2; (a) δ^T (b) δ^L. The Corey relative permeability parameters used are listed in Table 1. The components' properties are given in Tables 2 and 3.

one intermediate pseudocomponent (PC2), and two heavy pseudocomponents (PC3 and PC4). Their properties are given in Tables 2 and 3. The oil gravity is calculated to be approximately 10°API. The injection gas consists of 20 mol% PC1 and 80 mol% PC2. The reservoir temperature is 86°F. Detailed phase behavior predictions in P-T-x space for this quaternary fluid can be found in Okuno and Xu (2014a), and are not duplicated here.

Figure 1 presents simulated recoveries of PC3 and PC4 at five different pressures, 700, 800, 1000, 1500, and 1750 psia. The figure indicates that the miscibility level of oil displacement increases with decreasing pressure, as also shown by Okuno and Xu (2014a) with a different set of relative permeability parameters. Use of model 2 results in higher oil recovery than use of model 1, and the difference becomes more obvious with increasing pressure. The PC4 recovery at 1750 psia at breakthrough of the three-phase trailing edge is 84.88% with model 1, which is 5.04% lower than when model 2 is used.

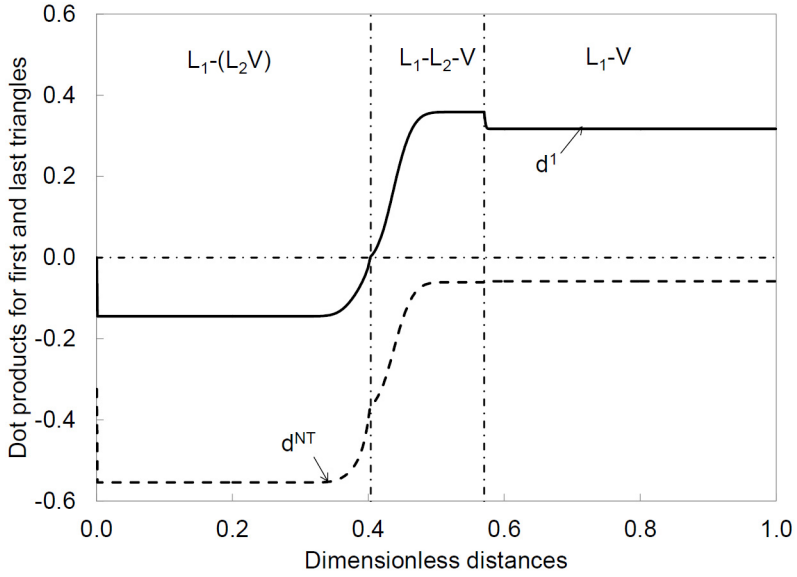

Figure 3—Dot products (equation 3) calculated at 0.3 PVI for the limiting tie triangles ($d^1 = d^{UCEP}$ and $d^{NT} = d^{LCEP}$) for the quaternary displacement at 1500 psia and 86°F with model 1. The oil and gas properties are given in Tables 2 and 3.

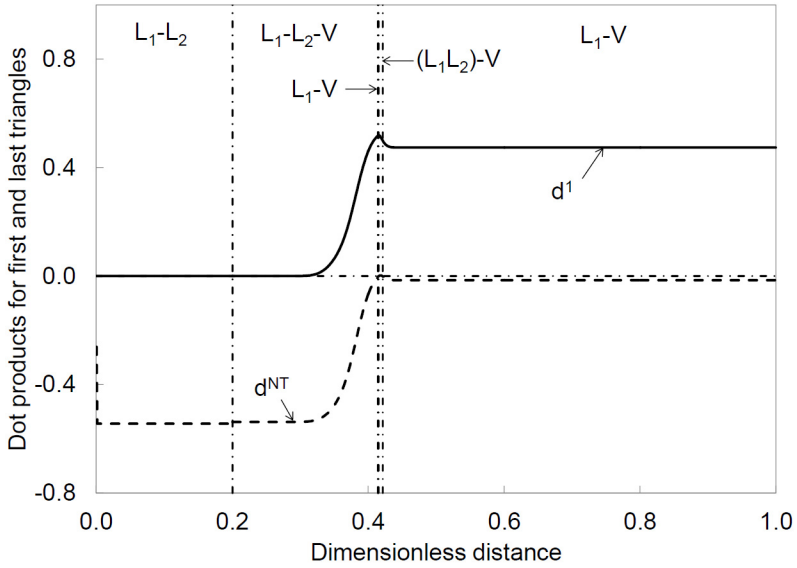

Figure 4—Dot products (equation 3) calculated at 0.3 PVI for the first and last triangles for the quaternary displacement at 700 psia and 86°F with the relative permeability model in Okuno and Xu (2014a). The oil and gas properties are given in Tables 2 and 3.

The degree of miscibility and phase mobilities affect oil displacements in a complicated manner. The distance parameters, δ^T and δ^L, were derived to understand the complicated interaction of flow and phase behavior through interphase mass transfer on multiphase transitions (Equations C-7 and C-8). Figure 2 shows the δ^T and δ^L parameters for the simulated displacements. The δ^T parameter accurately captures the oil displacement efficiency by three phases; i.e., the oil displacement becomes more efficient as δ^T decreases. As discussed in Okuno and Xu (2014ab), δ^L tends to be affected by numerical dispersion, especially for highly miscible displacements at 700 psia and 800 psia, because the leading edge of three phases exhibits drastic changes of components' concentrations (e.g., CO_2 or solvent components that form the L_2 phase with reservoir oil in simulation).

The effect of relative permeability on the oil displacement is more significant with increasing pressure because the degree of miscibility decreases with increasing pressure in this displacement. This is the first

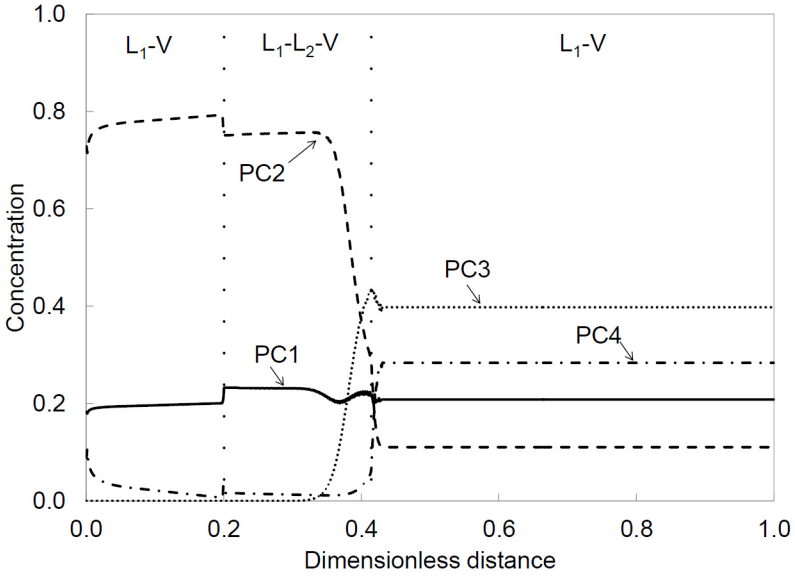

Figure 5—Concentration profiles at 0.3 PVI in the quaternary simulation at 700 psia with the conventional phase-identification method of Perschke et al. (1989). The Corey relative permeability parameters were taken from Okuno and Xu (2014a). The two phases upstream of the three-phase region are incorrectly labeled as L_1 and V because mass densities for the non-L_1 phase are calculated to be lower than the specified value, 30 lbm/ft^3.

Table 4—FLUID PROPERTIES FOR THE WEST SAK OIL (Xu 2012)

Components	Oil (Mol%)	Rich Gas (Mol%)	Lean Gas (Mol%)	Molecular Weight	Tc (°R)	Pc (psia)	Vc (ft^3/lb-mol)	Acentric Factor	Binary Interaction CO_2	Binary Interaction C_1
CO_2	0.22	0	0	44.01	547.56	1069.87	1.51	0.2250	0	0.18
C_1	27.47	0	84	16.04	343.08	667.20	1.59	0.0080	0.18	0
C_2	0.66	35	9	30.07	549.72	708.35	2.37	0.0980	0.18	0.010
C_3	0.15	34	6	44.10	665.64	615.76	3.25	0.1520	0.18	0.010
C_4	0.27	31	1	58.12	765.36	551.10	4.08	0.1930	0.18	0.010
C_5	0.19	0	0	72.15	845.28	489.38	4.87	0.2510	0.18	0.010
C_6	0.29	0	0	86.18	913.32	430.59	5.93	0.2960	0.18	0.010
C_{7-9}	3.22	0	0	105.65	1060.48	418.62	8.29	0.3697	0.05	0.007
C_{10-14}	17.95	0	0	157.72	1220.5	323.21	8.41	0.5389	0.05	0.007
C_{15-18}	13.21	0	0	210.19	1349.89	274.12	14.54	0.6992	0.05	0.007
C_{19-23}	10.91	0	0	259.06	1424.95	251.96	19.02	0.8373	0.05	0.007
C_{24-27}	5.84	0	0	302.85	1493.37	242.09	22.88	0.9500	0.05	0.007
C_{28-33}	6.60	0	0	344.37	1550.96	230.14	22.74	1.0453	0.05	0.007
C_{34-40}	4.42	0	0	389.77	1629.48	223.31	44.05	1.1345	0.05	0.007
C_{41+}	8.60	0	0	600.00	1914.78	182.82	53.57	1.2120	0.05	0.007

time the effect of relative permeability on three-hydrocarbon-phase oil displacement is confirmed by interphase mass transfer, which was not entirely possible without the reliable phase-identification algorithm developed in this research. The distance parameters can represent how components are redistributed on multiphase transitions in three-phase flow because they consider phase mobilities as well as phase compositions through mass conservation equations (Okuno and Xu 2014ab).

Figure 3 depicts d^1 and d^{NT} at 0.3 PVI in the simulation at 1500 psia with model 1. The first and N_T^{th} triangles in the table are the limiting triangles at UCEP and LCEP, respectively. Thus, $d^1 = d^{UCEP}$, and $d^{NT} = d^{LCEP}$ in this case. The two phases downstream of the three-phase region are L_1 and V. The subcritical state is clearly indicated by the signs of d^{UCEP} and d^{LCEP}. The two phases upstream of the three-phase region are L_1 and (L_2V), as can be confirmed by the negative d^{UCEP} and d^{LCEP}.

Figure 4 shows d^1 and d^{NT} at 0.3 PVI in the simulation at 700 psia. For this simulation, the relative-permeability parameters given in Okuno and Xu (2014a) were used. The first tie triangle in the

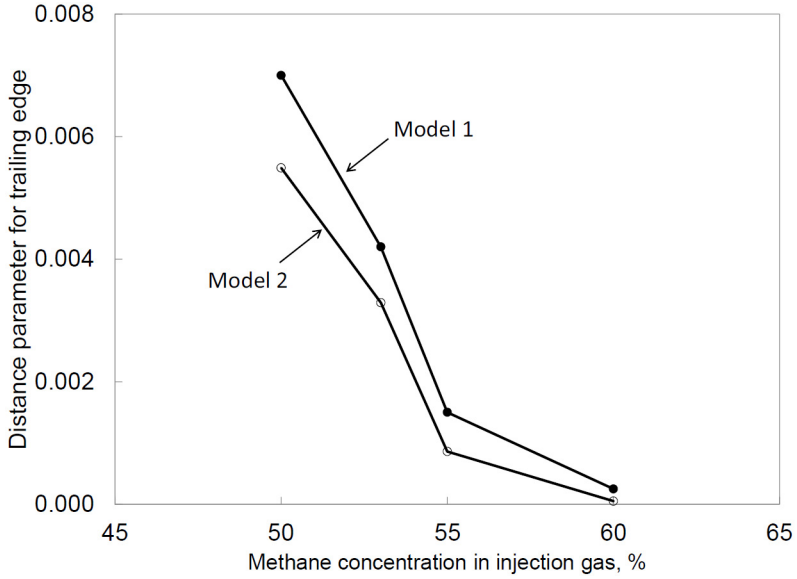

(a)

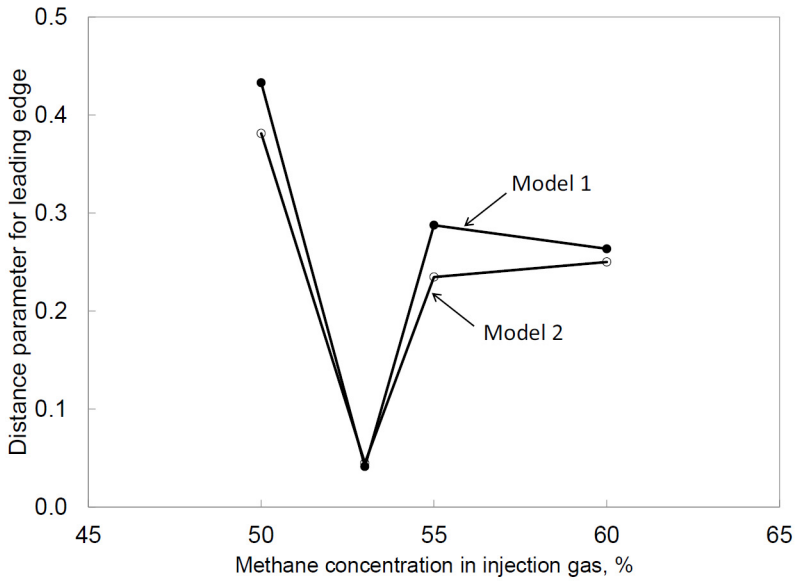

(b)

Figure 6—The δ^T and δ^L parameters (see Appendix C) for the West Sak oil displacements with relative permeability models 1 and 2; (a) δ^T (b) δ^L. The Corey relative permeability parameters used are listed in Table 1. The components' properties are given in Table 4.

tie-triangle table is on the PC3-free subspace since the UCEP does not exist in composition space at this pressure. The N_T^{th} tie triangle is the limiting tie triangle at the LCEP. The algorithm can clearly distinguish the super-LCEP state from the sub-CEP state of L_1-V in the downstream two-phase region by checking the sign of d^{LCEP}. The negative sign of d^{LCEP} indicates that the original oil is in the subcritical L_1-V region, as mentioned in Okuno and Xu (2014b). Then, the composition path goes to the super-LCEP region [(L_1L_2)-V] before entering the three-phase region through the L_1-V edge of a tie triangle. This seems to be a numerical artifact due to a small increase of the PC3 concentration that is simulated just downstream of the three-phase region.

Figure 5 shows the concentration profiles for the same simulation case as Figure 4, but with the conventional phase identification of Perschke et al. (1989). The two phases upstream of the three-phase region are incorrectly labeled as L_1 and V because mass densities for the non-L_1 phase are calculated to

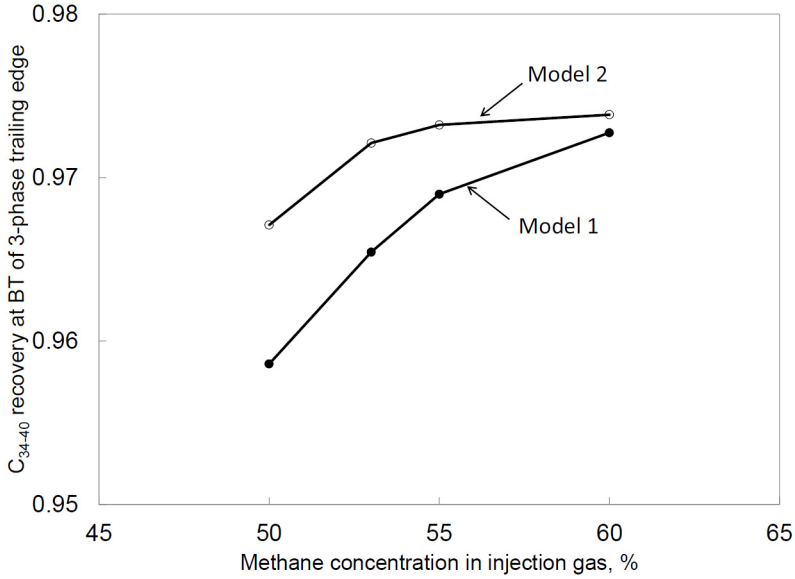

Figure 7—C_{34-40} recoveries simulated for the West Sak oil displacements at 1500 psia and 65°F by use of relative permeability models 1 and 2. The fluid properties are given in Table 4. Methane dilution enables to increase the miscibility level of this West Sak oil displacement by making interphase mass transfer on multiphase transitions more favorable (see Figure 6a). The increased miscibility level can be so high that relative permeability parameters little affect oil recovery predictions.

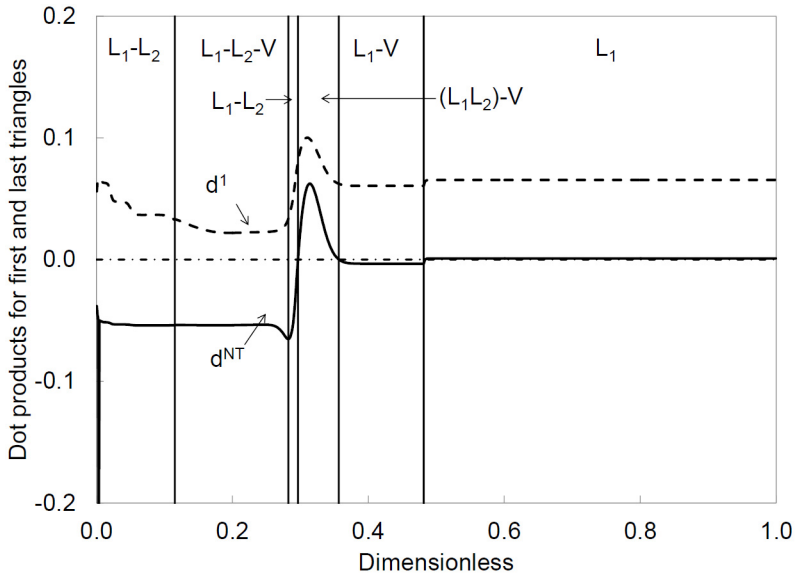

Figure 8—Dot products (equation 3) calculated at 0.3 PVI for the first and last triangles for the West Sak oil displacement at 55%-methane-dilution at 1500 psia and 65°F with relative permeability model 1. The oil and gas properties are given in Table 4.

be lower than the specified value, 30 lbm/ft^3. The small increase in the PC3 concentration ahead of the three-phase region also occurs in this case, but the conventional phase identification does not precisely detect the phase transitions depicted in Figure 4 with the new phase-identification method.

A sensitivity analysis for N_T indicated that the minimum N_T required is four for this case. The small N_T required is likely because the N_C used is small and because the non-linearity of the $\vec{n}$ trajectory is insignificant.

West Sak Oil Displacement

The West Sak oil model used consists of 15 components, which include eight pseudocomponents for the C_{7+} fraction (Xu 2012). Their properties are given in Table 4. Okuno and Xu (2014a) used this fluid

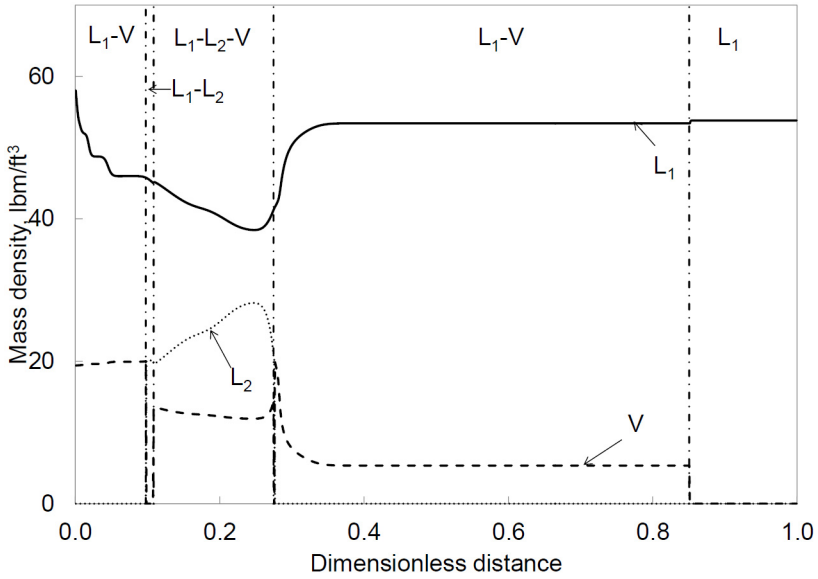

Figure 9—Mass density profiles at 0.3 PVI for the West Sak oil displacement at 55%-methane-dilution at 1500 psia at 65°F. The relative permeability parameters were taken from Okuno and Xu (2014a). The conventional phase-identification method is used with a threshold mass density of 20 lbm/ft^3. The two-phase region downstream of the three-phase region is labeled as L_1-V, and discontinuities occur in the upstream two-phase region.

model to explain the nonmonotonic oil recovery at 1.2 PVI with respect to gas enrichment reported by DeRuiter et al. (1994) and Mohanty et al. (1995). The oil gravity is calculated to be approximately 21°API. The reservoir temperature is 65°F. Phase behavior predictions for this fluid can be found in Okuno and Xu (2014a).

The injection gas consists of two gaseous mixtures: the rich-gas mixture of 35 mol% ethane, 34 mol% propane, and 31 mol% n-butane, and the lean-gas mixture of 84 mol% methane, 9 mol% ethane, 6 mol% propane, and 1 mol% n-butane. Oil displacements are simulated for four different enrichment levels. The resulting enriched gases are referred to by use of their methane concentrations. The simulations are performed at 50%-, 53%-, 55%-, and 60%-methane-dilution at 1500 psia.

Figure 6 shows the distance parameters, δ^T and δ^L, calculated in the simulations with relative permeability models 1 and 2. δ^T clearly indicates that the miscibility level of oil displacement increases with increasing methane dilution, which is consistent with results given in the literature (DeRuiter et al. 1994; Mohanty et al. 1995; Okuno and Xu 2014a). It also shows that use of model 2 results in interphase mass transfer on the multiphase transition that is more favorable in terms of oil displacement by three phases. The difference between models 1 and 2 decreases with increasing methane dilution. These results can be confirmed in Figure 7, which presents recoveries of C_{34}-$_{40}$ at breakthrough of the trailing edge of three phases. Similar trends were also observed for other heavy components. Thus, methane dilution enables to increase the miscibility level of this West Sak oil displacement by making interphase mass transfer on multiphase transitions more favorable. The increased miscibility level can be so high that relative permeability parameters little affect oil recovery predictions. Further investigation is required to understand under what conditions methane dilution can enhance the miscibility of oil displacement. As in the previous case and a few of the simulation cases in Okuno and Xu (2014ab), however, δ^L fluctuates for highly miscible displacements and may not be a good indicator of the oil displacement efficiency by three phases in the presence of numerical dispersion.

Figure 8 shows d^{UCEP} and d^{LCEP} at 0.3 PVI in the simulation at 55%-methane-dilution with model 1. The two phases downstream of the three-phase region change their identities; L_1-V, (L_1L_2)-V, and L_1-L_2 in the direction from the producer to the injector. The algorithm developed can precisely identify phases even in this complex simulation case. The complexity of phase identification tends to increase with increasing N_C. The minimum N_T required for the West Sak oil case is seven.

Figure 9 shows failures of phase identification by the conventional method when used in the West Sak oil displacement at 55%-methane-dilution at 0.3 PVI. The threshold mass density used is 20 lbm/ft^3. For this simulation, the relative-permeability parameters given in Okuno and Xu (2014a) were used. The two phases downstream of the three-phase region are labeled as L_1 and V, and no distinction is made between the sub- and super-critical states. The two-phase region upstream of the three-phase region exhibits discontinuities. This is one of the typical failures caused by using a mass-density threshold.

Conclusions

This paper presented the effect of relative permeability on oil displacement by three hydrocarbon phases. A new method for robust phase identification was developed and successfully applied to numerical simulations of 1D convective flow with three hydrocarbon phases. Simulation results were analyzed by use of the distance parameters that describe interphase mass transfer on multiphase transitions in oil displacement. Conclusions are as follows:

1. The phase-identification method developed in this research can correctly solve for equilibrium-phase identities, which are part of the solution for a multiphase flow problem. The robustness comes mainly from the capability of precise quantification of the location of the current overall composition relative to the three-phase region in composition space. The method can distinguish the super-CEP states from the sub-CEP states by use of the critical tie-triangle extensions. With the developed method, five types of two-phase regions can be properly considered around the three-phase region in three-hydrocarbon-phase flow simulation.
2. In the simulation cases with the quaternary fluid and the West Sak oil, the analytical result of interphase mass transfer presented by Okuno and Xu (2014ab) was validated with varying level of miscibility and different relative-permeability parameters. The distance parameters can properly represent the interaction of flow and phase behavior since they were derived from mass conservation, not only from thermodynamic conditions. Results showed that the distance parameter for the trailing edge (Equation C-7) can accurately quantify the oil displacement efficiency by three hydrocarbon phases even in numerical simulation. The distance parameter for the leading edge (equation C-8) tends to be affected by numerical dispersion especially in highly miscible displacements, as also shown in Okuno and Xu (2014ab) with the UTCOMP simulator.
3. The simulation case study for the West Sak oil confirmed the experimental observation of DeRuiter et al. (1994) and Mohanty et al. (1995). The analysis of interphase mass transfer indicated that the miscibility level of oil displacement increases with increasing methane dilution in this case. The effect of relative permeability diminishes as the miscibility level increases owing to methane dilution. Further investigation is required to understand under what conditions methane dilution can enhance miscibility development in oil displacement.

Nomenclature

c_{ij}	: Volumetric fraction of component i in phase j
$\underline{c}_j$	: Vector consisting of c_{ij} as defined in Equation C-4
C_i	: Overall volume fraction of component i
d	: Composition distance
f_j	: Fractional flow of phase j
F_i	: Overall fractional flow of component i
k	: Gridblock index
L_1	: Oleic phase
L_2	: Solvent-rich liquid phase
(L_1L_2)	: Supercritical phase in super-LCEP region

(L_2V) : Supercritical phase in super-UCEP region
m : Index for tie triangles in Equation (3)
n : Time-step index in Equation (C-3) or outward unit normal vector in Equation (C-2)
$\vec{n}$: Unit normal vector in Equations (1), (2) and (3)
N_j (j=1, 2, or 3) : Non-oleic phase (i.e., L_2 or V)
N_C : Number of components
N_P : Number of phases
N_T : Number of tie triangles
P_C : Critical pressure
S : Surface area of control volume
S_j : Saturation of phase j
T_C : Critical temperature
t_D : Dimensionless time in pore volumes
v_D : Dimensionless velocity
V : Gaseous phase or control volume in Equation C-2
V_C : Critical volume
$\vec{x}$: Composition vector in Equation (1)
x_D : Dimensionless distance from the injector
$\underline{x}_j$: Composition vector of phase j in Equation (C-5)
$\vec{z}$: Vector of overall composition
$\underline{z}^{int}$: Intersection composition

Nomenclature

D : Downstream
U : Upstream

Nomenclature

γ : Parameter defined in Equation C-4
Γ : Parameter defined in Equations C-5
δ : Distance defined in Equations C-7 and C-8

Nomenclature

BT : Breakthrough
CEP : Critical endpoint
EOS : Equation of state
LCEP : Lower critical endpoint
MCM : Multicontact miscibility
PVI : Pore-volume injected
PC : Pseudo component
PR : Peng-Robinson
UCEP : Upper critical endpoint

Acknowledgements

This research was financially supported by research grants from the Natural Sciences and Engineering Research Council of Canada (RGPIN 418266), Japan Petroleum Exploration Co., Ltd. (JAPEX), and Japan Canada Oil Sands Ltd. (JACOS). Zhongguo Xu has received a scholarship from the China Scholarship Council. We gratefully acknowledge these supports.

References

Beygi, M.R., Delshad, M., Pudugramam, V.S., Pope, G.A., and Wheeler, M.F. 2014. Novel Three-Phase Compositional Relative Permeability and Three-Phase Hysteresis Models. *SPE Journal* (in print). SPE-165324-PA.

Bruining, J. and Marchesin, D. 2007. Maximal Oil Recovery by Simultaneous Condensation of Alkane and Steam, *Physical Review E* **75**(3): 036312-1–036312-16.

Chang. Y.-B. 1990. *Development and Application of an Equation of State Compositional Simulator*. PhD dissertation, the University of Texas at Austin, Austin, Texas.

Chang, Y.-B., Pope, G.A., and Sepehrnoori, K. 1990. A Higher-Order Finite-Difference Compositional Simulator. *Journal of Petroleum Science and Engineering* **5**(1): 35–50.

Corey, A., Rathjens, C., Henderson, J., et al 1956. Three-Phase Relative Permeability. *Journal of Petroleum Technology* **8**(11): 63–65. SPE-737-G.

Creek, J.L. and Sheffield, J.M. 1993. Phase Behavior, Fluid Properties, and Displacement Characteristics of Permian Basin Reservoir Fluid/CO2 Systems. *SPE Reservoir Engineering* **8**(1): 34–42. SPE-20188-PA.

DeRuiter, R.A., Nash, L.J., and Singletary, M.S. 1994. Solubility and Displacement Behavior of a Viscous Crude with CO2 and Hydrocarbon Gases. *SPE Reservoir Engineering* **9**(2): 101–106. SPE-20523-PA.

Dindoruk, B. 1992. *Analytical Theory of Multiphase, Multicomponent Displacement in Porous Media*. PhD dissertation, Stanford University, Stanford, CA.

Gardner, J.W., Orr, Jr., F.M., and Patel, P.D. 1981. The Effect of Phase Behavior on CO2-Flood Displacement Efficiency. *Journal of Petroleum Technology* **33**(11): 2067–2081. SPE-8367-PA.

Glandt, C.A. and Chapman, W.G. 1995. The Effect of Water Dissolution on Oil Viscosity. *SPE Reservoir Engineering* **10**(1): 59–64. SPE-24631-PA.

Guler, B., Wang, P., Delshad, M., et al 2001. Three- and Four-Phase Flow Compositional Simulations of CO2/NGL EOR. Presented at the SPE Annual Technical Conference and Exhibition, New Orleans, Louisiana, 30 September-3 October. SPE-71485-MS.

Helfferich, F.G. 1979. General Theory of Multicomponent, Multiphase Displacement. *SPE Journal* **21**(01): 51–62. SPE-8372-PA.

Iranshahr, A., Voskov, D., and Tchelepi, H.A. 2012. Tie-Simplex-Based Compositional Space Parameterization: Continuity and Generalization to Multiphase Systems. *AIChE Journal* **59**(5): 1684–1701.

Iranshahr, A., Voskov, D., and Tchelepi, H.A. 2013. A Negative-Flash Tie-Simplex Approach for Multiphase Reservoir Simulation. *SPE Journal* **18**(6): 1140–1149. SPE-141896-PA.

Johns, R.T. 1992. *Analytical Theory of Multicomponent Gas Drives with Two-Phase Mass Transfer*. PhD dissertation, Stanford University, Stanford, CA.

Knobler, C.M. and Scott, R.L. 1984. Multicritical Points in Fluid Mixtures: Experimental Studies. In *Phase Transitions and Critical Phenomena* vol. **9,** ed. Domb, C. and Lebowitz, J.L., Chapter 2, 163–231. Academic Press, London.

Kumar, A. and Okuno, R. 2013. Characterization of Reservoir Fluids using an EOS Based on Perturbation from n-Alkanes, *Fluid Phase Equilibria* **358**: 250–271.

LaForce, T.C. 2012. Insight from Analytical Solutions for Improved Simulation of Miscible WAG Flooding in One Dimension. *Computational Geosciences* **16**(4): 1007–1020.

LaForce, T.C., and Jessen, K. 2010. Analytical and Numerical Investigation of Multicomponent Multiphase WAG Displacements. *Computational Geosciences* **14**(4): 745–754.

LaForce, T.C., Jessen, K., and Orr, Jr., F.M. 2006. Analytical Solutions for Compositional Three-Phase Four-Component Displacements. Presented at SPE ATCE, San Antonio, Texas, USA, 24-27 September. SPE-102777-MS.

LaForce, T.C., Jessen, K., and Orr, Jr., F.M. 2008a. Four-Component Gas/Water/Oil Displacements in One Dimension: Part I. Structure of the Conservation Law. *Transport in Porous Media* **71**: 199–216.

LaForce, T.C., Jessen, K., and Orr, Jr., F.M. 2008b. Four-Component Gas/Water/Oil Displacements in One Dimension: Part II. Example Solutions. *Transport in Porous Media* **72**: 83–96.

LaForce, T.C., and Johns, R.T. 2005a. Analytical Solutions for Surfactant-Enhanced Remediation of Nonaqueous Phase Liquids. *Water Resources Research* **41**(10): 1–14. W10420.

LaForce, T.C., and Johns, R.T. 2005b. Composition Routes for Three-Phase Partially Miscible Flow in Ternary Systems. *SPE Journal* **10**(02): 161–174. SPE-89438-PA.

LaForce, T.C., and Johns, R.T. 2009. Effect of Initial Gas Saturation on Miscible Gasflood Recovery. *Journal of Petroleum Science and Engineering* **70**(3-4): 198–203.

LaForce, T.C., and Orr, Jr., F.M. 2008. Development of Gas/Oil Miscibility in Water and Gas Injection. Presented at SPE ATCE, Denver, Colorado, USA, 21-24 Sep. SPE-116119-MS.

Lake, L.W. 1989. *Enhanced Oil Recovery*. First Edition, Prentice Hall, Upper Saddle River, N.J.

Li, L., Khorsandi, S. and Johns, R.T. 2014. Multiple Mixing Cell Method for Three-Hydrocarbon-Phase Displacements. Presented at the SPE IORS, Tulsa, Oklahoma, USA, 12-16 April. SPE-169150-MS.

Lohrenz, J., Bray, B.C., and Clark, C.R. 1964. Calculating Viscosities of Reservoir Fluids from Their Compositions. *Journal of Petroleum Technology* **16**(10): 1171–1176.

Luo, S. and Barrufet, M.A. 2005. Reservoir Simulation Study of Water-in-Oil Solubility Effect on Oil Recovery in Steam Injection Process. *SPE Reservoir Evaluation and Engineering* **8**(6): 528–533. SPE-89407-PA.

Metcalfe, R.S. and Yarborough, L. 1979. The Effect of Phase Equilibria on the CO2 Displacement Mechanism. *SPE Journal* **19**(4): 242–252. SPE-7061-PA.

Mohanty, K.K., Masino, Jr., W.H., Ma, T.D., and Nash, L.J. 1995. Role of Three-Hydrocarbon-Phase Flow in a Gas-Displacement Process. *SPE Reservoir Engineering* **10**(3): 214–221. SPE-24115-PA.

Okuno, R. 2009. *Modeling of Multiphase Behavior for Gas Flooding Simulation*. PhD dissertation, the University of Texas at Austin, Austin, Texas.

Okuno, R., Johns, R.T., and Sepehrnoori, K. 2010. A New Algorithm for Rachford-Rice for Multiphase Compositional Simulation, *SPE Journal* **15**(2): 313–325. SPE-117752-PA.

Okuno, R., Johns, R.T., and Sepehrnoori, K. 2011. Mechanisms for High Displacement Efficiency of Low-Temperature CO2 Floods. *SPE Journal,* **16**(4): 751–767. SPE-129846-PA.

Okuno, R. and Xu, Z. 2014a. Efficient Displacement of Heavy Oil by Use of Three Hydrocarbon Phases. *SPE Journal* **19**(5): 956–973. SPE-165470-PA.

Okuno, R. and Xu, Z. 2014b. Mass Transfer on Multiphase Transitions in Low-Temperature Carbon-Dioxide Floods, *Accepted for publication in SPE Journal* on February 5, 2014. SPE-166345-PA.

Orr, Jr., F.M. 2007. *Theory of Gas Injection Processes*. Tie-Line Publications, Holte, Denmark.

Orr, Jr., F.M. and Jensen, C.M. 1984. Interpretation of Pressure-Composition Phase Diagrams for CO2/Crude-Oil Systems. *SPE Journal* **24**(5): 485–497. SPE-11125-PA.

Peng, D.-Y. and Robinson, D.B. 1976. A New Two-Constant Equation of State. *Industrial & Engineering Chemistry Fundamentals* **15**(1): 59–64.

Perschke, D.R. 1988. *Equation of State Phase Behavior Modeling for Compositional Simulation*. PhD dissertation, University of Texas at Austin, Austin, Texas.

Perschke, D.R., Pope, G.A., and Sepehrnoori, K. 1989. *Phase Identification During Compositional*

Simulation. SPE-19442-MS.

Peters, C.J. 1994. Multiphase Equilibria in Near-Critical Solvents. E. Kiran and J.M.H. Levelt Sengers (eds.), *Supercritical Fluids,* 117–145. Kluwer Academic Publishers.

Voskov, D. and Tchelepi, H.A. 2009a. Compositional Space Parameterization: Theory and Application for Immiscible Displacement. *SPE Journal* **14**(3): 431–440. SPE-106029-PA.

Voskov, D. and Tchelepi, H.A. 2009b. Compositional Space Parameterization: Multicontact Miscible Displacements and Extension to Multiple Phases. *SPE Journal* **14**(3): 441–449. SPE-113492-PA.

Xu, Z. 2012. *Displacement Efficiency of Solvent Floods with Three Partially Miscible Phases*. MEng project report, the University of Alberta, Edmonton, Alberta (June 2012).

Yuan, C. and Pope, G.A. 2012. A New Method to Model Relative Permeability in Compositional Simulators to Avoid Discontinuous Changes Caused by Phase-Identification Problems. *SPE Journal* **17**(4): 1221–1230. SPE-142093-PA.

Appendix A

Schematic of a Three-Phase Region Bounded by Critical Endpoint Tie Lines

A three-phase region has one degree of freedom at a given temperature and pressure for four components. Therefore, a three-phase region is a volumetric region in a quaternary diagram. The three-phase region consists of an infinite number of tie triangles. A tie triangle changes its shape and size within the three-phase region. Two tie triangles are shown to illustrate tie triangles exhibiting near-CEP behavior. A CEP is not a point in composition space, but is a tie line (or a limiting tie triangle) in which two of the three phases are critical in the presence of the other noncritical phase. The UCEP typically occurs at higher solvent concentrations than the LCEP as observed for CO_2-n-alkane and n-alkane binaries. More details on three-hydrocarbon-phase behavior predictions are given in Okuno (2009).

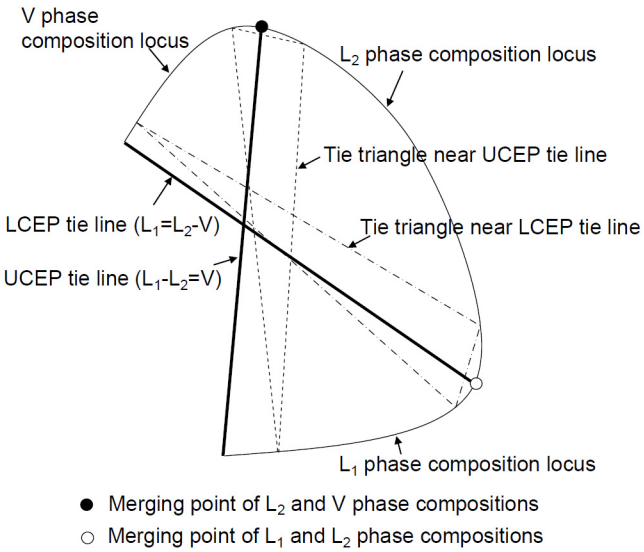

Figure A-1—Schematic of a three-phase region bounded by critical endpoint (CEP) tie lines for a quaternary system at a fixed temperature and pressure.

Appendix B

Schematics of Phase Behavior in Two- and Three-Phase Displacements

A two-phase displacement involves the L_1 phase and a non-oleic (N_1) phase. Although the N_1 phase is often the V phase because of a fast traveling methane bank, we do not specify its phase identity in the schematic for generality. A phase transition between one and two phases occurs at the displacement front, where the N_1 phase appears. Complete evaporation of the L_1 phase is invisible in the schematic as the evaporation wave is normally much slower than the displacement front, especially in the presence of dispersion.

Phase behavior for three-phase displacement of oil is more involved. Two non-oleic phases appear in sequence in the direction from the producer to the injector. The non-oleic phase that appears first at the displacement front is referred to as N_1. The N_2 phase then appears at the leading edge of the three-phase region, which is at equilibrium with the L_1 and N_1 phases in the three-phase region. One of the two non-oleic phases disappears at the trailing edge of the three-phase region. The non-oleic phase that coexists with the L_1 phase in the upstream two-phase region is referred to as N_3, which is either N_1 or N_2 depending on the phase transition there.

There are four patterns for phase transitions for the three-phase displacement in Figure B-1 since the N_1-N_3 pair can be either V-V, or V-L_2, or L_2-V, or L_2-L_2. That is, the four patterns for (N_1, N_2, N_3) are as follows: (V, L_2, V), (V, L_2, L_2), (L_2, V, V), and (L_2, V, L_2). The two phases at the displacement front is typically the V and L_1 phases because of a fast travelling methane bank. For the two phases upstream of the three-phase region, however, both L_1-V and L_1-L_2 are common depending on phase behavior near the injection gas composition at the operating temperature and pressure. Although it is possible to have a direct transition between one phase and three phases without involving two-phase equilibrium, this type of phase transition is not considered in this research.

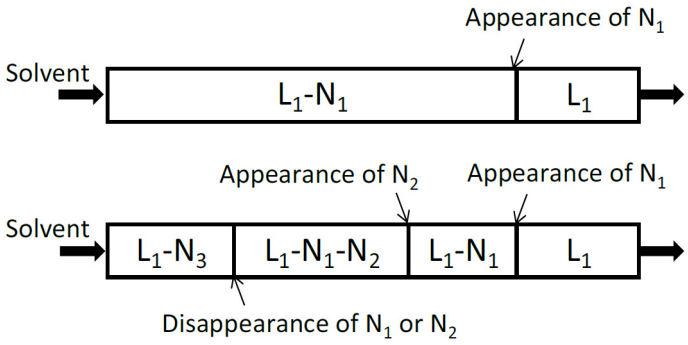

Figure B-1—Schematics of phase behavior in two- and three-phase displacements. The oleic phase is given as L_1. A non-oleic phase (N_1) appears at the displacement front for two- and three-phase displacements. For a three-phase displacement, another non-oleic phase (N_2) appears at the leading edge of the three-phase region. One of the two non-oleic phases (N_1 and N_2) in the three-phase region disappears at the trailing edge of the three-phase region. The non-oleic phase (N_3) in the upstream two-phase region is either N_1 or N_2 depending on the phase behavior involved there.

Appendix C

Mass Conservation Equations and Interphase Mass Transfer on Multiphase Transitions

Conservation of mass for a component in N_P-phase flow through porous media is considered with the following assumptions:

– One dimensional flow with no gravity
– Constant temperature
– Change in pressure is small over the displacement length
– Constant porosity with time
– No diffusion/dispersion
– No chemical reaction or sorption on the solid phase
– No capillary pressure
– Local equilibrium
– Ideal mixing
– Laminar flow.

We then obtain

$$\frac{\partial C_i}{\partial t_D} + \frac{\partial F_i}{\partial x_D} = 0, \tag{C-1}$$

where t_D is the dimensionless time measured in pore volumes, x_D is the dimensionless distance from the injector, C_i is the overall volume fraction of component i, F_i is the overall fractional flow of component i, and $i = 1, 2, \ldots, (N_C - 1)$. C_i and F_i are given as

$$C_i = \sum_{j=1}^{N_P} S_j c_{ij}$$

$$F_i = \sum_{j=1}^{N_P} f_j c_{ij}.$$

where S_j is the saturation of phase j, f_j is the fractional flow of phase j, and c_{ij} is the volume fraction of component i in phase j. A detailed derivation of Equation C-1 is given in Orr (2007).

The weak form of Equation C-1 is

$$\frac{d}{dt_D}\int C_i \, dV + \int n \cdot F_i \, dS = 0, \tag{C-2}$$

where V and S are the volume and surface area of the control volume of interest, respectively. n is the outward normal unit vector on surface S. The explicit discretization of Equation C-2 by use of the one-point upstream weighting for the flux term yields

$$(C_i)_k^{n+1} = (C_i)_k^n + (\Delta t_D / \Delta x_D)[(F_i)_{k-1}^n - (F_i)_k^n], \tag{C-3}$$

where n is the time-step index and k is the gridblock index. Δx_D and Δt_D are the gridblock size and time-step size, respectively, which are uniform in this research. Equation C-3 is used in the simulations in the current paper.

Suppose a phase transition between $N_P{}^U$ phases and $N_P{}^D$ phases propagates at a dimensionless velocity of v_D. $N_P{}^U$ and $N_P{}^D$ are the numbers of phases upstream and downstream of the phase transition. Then, discretized mass-conservation equations on the phase transition are

$$\sum_{j=1}^{N_P^U} \gamma_j^U \underline{c}_j^U = \sum_{j=1}^{N_P^D} \gamma_j^D \underline{c}_j^D. \tag{C-4}$$

where $\underline{c}_j$ is a vector consisting of c_{ij}, $\gamma_j^U = (v_D S_j^U - f_j^U)/(v_D - 1)$, and $\gamma_j^D = (v_D S_j^D - f_j^D)/(v_D - 1)$. Note that $\sum_{j=1}^{N_P^U} \gamma_j^U = 1.0$ and $\sum_{j=1}^{N_P^D} \gamma_j^D = 1.0$.

Equation C-4 is of the identical form with the generalized jump conditions on multiphase transition presented in Okuno and Xu (2014a). The difference is that v_D in Equation C-4 is, in general, not the same as the shock velocity of the corresponding multiphase transition in the MOC solution. Equation C-4 states that components are redistributed on a multiphase transition through an intersection of the tie simplex extension of $(N_P{}^D - 1)$ dimensions with that of $(N_P{}^U - 1)$ dimensions. Equation C-4 can be used for mechanistic interpretation of mass transfer on a multiphase transition even in the presence of numerical dispersion.

Equation C-5 in composition space is

$$\underline{z}^{int} = \sum_{j=1}^{N_P^U} \Gamma_j^U \underline{x}_j^U = \sum_{j=1}^{N_P^D} \Gamma_j^D \underline{x}_j^D \quad \text{(C-5)}$$

where $\sum_{j=1}^{N_P^U} \Gamma_j^U = \sum_{j=1}^{N_P^D} \Gamma_j^D = 1.0$. The intersection composition is $\underline{z}^{int}$. The Γ parameters give the relative location of $\underline{z}^{int}$ with respect to the corresponding tie simplex. For example, the Γ_j^U parameters give the location of $\underline{z}^{int}$ relative to the tie simplex defined by N_P^U phase compositions $\underline{x}_j$, where $j = 1, 2, \ldots, N_P^U$.

Okuno and Xu (2014b) presented that MCM between the L_1 and L_2 phases in three-hydrocarbon-phase flow can be developed on a LCEP tie line, where the non-V phase switches its identity from L_1 to L_2 with no three-phase equilibrium involved. When this occurs, the following three distances are zero:

$$d_{L1-L2} = \left\| \underline{x}_{L_1} - \underline{x}_{L_2} \right\|_2 \quad \text{(C-6)}$$

$$\delta^L = \left\| \Gamma_{N_1}^U \underline{x}_{N_1}^U - \Gamma_{N_1}^D \underline{x}_{N_1}^D \right\|_2 \quad \text{(C-7)}$$

$$\delta^T = \left\| \Gamma_{L_1}^U \underline{x}_{L_1}^U - \Gamma_{L_1}^D \underline{x}_{L_1}^D \right\|_2. \quad \text{(C-8)}$$

Equations C-6 and C-7 are defined at the leading edge of the three-phase region, and Equation C-8 is at the trailing edge. $d_{L1\text{-}L2}$ is a criticality measure for a LCEP. δ^L and δ^T quantify the deviation from the ideal interphase mass transfer (in terms of oil displacement by three phases) on the phase transitions at the leading and trailing edges of three hydrocarbon phases, respectively. At the limit of three-phase flow, the interphase mass transfer occurs in the ideal manner; $\delta^L = \delta^T = 0$. Detailed discussions on these equations can be found in Okuno and Xu (2014ab).

CONVERSION FACTORS

ft × 3.048*	E-01	= m
°F (°F – 32)/1.8		= °C
psi × 6.894 757	E+00	= kPa

*Conversion factor is exact.